PHYSICAL REVIEW B VOLUME 23, NUMBER 9 1 MAY 1981

Satellite structure in photoelectron and Auger spectra of copper dihalides

G. van der Laan, C. Westra, C. Haas, and G. A. Sawatzky
*Laboratory of Inorganic Chemistry and Laboratory of Physical Chemistry, The University of Groningen,
Nijenborgh 16, 9747 AG Groningen, The Netherlands*
(Received 28 July 1980)

The satellite structure of core photoelectron and Auger lines of the copper dihalides are explained in terms of final-state energies diminished by Coulomb interactions between the valence electrons and the created core hole or holes. The satellite structure in the $3p$ and valence-band photoelectron spectra are shown to originate from the same final states as the $L_3M_{23}M_{45}$ and $L_3M_{45}M_{45}$ main Auger lines. The energies of the main core lines are shown to yield information about the valence ligand binding energies and therefore are sensitive to chemical shifts. The satellite lines are rather insensitive to chemical shifts but their intensities yield information concerning the relative positions of the Cu $3d$ and ligand valence holes and the amount of hybridization. In terms of the core line photoelectron and Auger spectra we show that an assignment can be made of the valence-band spectra. From a combination of all the results we conclude that especially $CuCl_2$ and $CuBr_2$ are strongly covalent and we predict that in CuI_2 the valence hole would be predominantly in the I $5p$ level which is probably the reason why this material is not stable.

I. INTRODUCTION

The x-ray photoelectron spectra of divalent copper compounds are known to exhibit strong satellite structure in contrast to those of monovalent copper compounds.[1] These satellites are due to the interaction between the core hole and the valence electrons resulting in a change in the potential seen by the valence electrons upon the creation of the core hole. In the sudden approximation[2] this results in satellite structure, with the intensities of the lines in the monopole approximation given by the square of the overlap between the frozen initial-state wave function and the possible final-state eigenfunctions for the N-1 electron system. These overlap integrals are zero unless the symmetry of the final-state and the frozen-state wave functions are the same. Because of this, only some transitions are possible like a $3d \rightarrow 4s$ transition and charge transfer transitions. Yin *et al.*[3] have pointed out that a $3d-4s$ transition is not possible for a d^{10} configuration, but can occur in d^9. In all the copper dihalides, the copper site has D_{4h} symmetry, with the ground state of the divalent copper ion (d^9) belonging to a B_{1g} representation. The B_{1g} representation is also present in a $3d^8\,4s^1$ configuration and therefore a satellite corresponding to this final state may be present. One would however expect this to be a wide line because of the width of the $4s$ band, unless it is a bound state. Aside from this we would also expect to see a large multiplet splitting corresponding to a $3d^8$ configuration.

Wallbank *et al.*[4] and Kim[5] propose a charge transfer transition from the ligand to the metal atom to explain the satellite structure. This would quite naturally explain the absence of satellite structure for a filled $3d$ shell.

It is however difficult to explain the energetics of the satellites unless one explicitly includes the strong interaction of the core hole with the valence electrons. In fact, as we will show below, this will for copper at least invert the identification of the satellite and main line, with the former corresponding to a $3d^9$-like state and the main line to a $3d^{10}$-like final state (i.e., the charge transfer state). Larsson[6,7] includes the interaction with the core hole and proposes that the satellite line corresponds to $3d^9$ and the main line to a $3d^{10}$ configuration. This also at least qualitatively explains the multiplet splitting observed in the satellite lines. This model is very similar to that used by Kotani and Toyozawa[8] for metals. Also Asada and Sugano[9] have recently proposed a similar model using numerical Hartree-Fock calculations of the energy levels in the initial and final states.

Multiplet splitting has also been suggested as a possible explanation for the structure in the spectra, but this has been shown to be much too small[10] to be able to explain the satellite main peak splittings.

It turns out that there is a rather simple way of checking the interpretation of the satellite structure in divalent copper compounds, at least for the $3d$ photoelectron lines, using a combination of x-ray photoelectron spectroscopy (XPS) and Auger spectros-

TABLE I. Binding energies in eV of the copper dihalides (reference binding energy C 1*s* is 284.6 eV).

		CuF_2	$CuCl_2$	$CuBr_2$
Ligand	F 2*s*, Cl 3*s*, Br 4*s*	31.6	17.5	15.8
	Cl 2*p*		199.8	
	F 1*s*, Cl 2*s*, Br 3*s*	685.7	269.8	255.9
	Br 3*d*			68.7
$\underline{\mathrm{Cu}\,3d}$ main:	$(3d^9\underline{L})+(3d^{10}\underline{L}^2)$	8.1	6.0	4.3
sat:	$(3d^8, {}^3F)$	. . .	12.0	10.5
	$(3d^8, {}^1G)$	~13.6	14.5	13.3
$\underline{\mathrm{Cu}\,3p}$ main:	$(\underline{3p}3d^{10}\underline{L})$	79.6	78.0	76.5
sat:	$(\overline{\underline{3p}}3d^9, {}^3D+{}^3P)$	85.6	86.4	86.1
	$(\overline{\underline{3p}}3d^9, {}^1F+{}^1P)$	94.0	94.2	92.9
$\underline{\mathrm{Cu}\,3s}$ main:	$(\underline{3s}3d^{10}\underline{L})$	126.8	125.4	123.1
sat:	$(\underline{3s}3d^9, {}^3D)$	. . .	131.8	130.5
	$(\underline{3s}3d^9, {}^1D)$	132.2	134.8	133.5
Cu $2p_{3/2}$ main:	$(\underline{2p}_{3/2}3d^{10}\underline{L})$	936.6	934.6	933.1
sat:	$(\underline{2p}_{3/2}3d^9)$	943.8	942.0	941.5
			944.6	943.1
Cu $2p_{1/2}$ main:	$(\underline{2p}_{1/2}3d^{10}\underline{L})$	956.4	954.4	952.9
sat:	$(\underline{2p}_{1/2}3d^9)$	963.4	963.2	962.9

copy. In this paper we show that these results are consistent with the interpretation of Larsson[7] and we develop a simple model which describes the physics involved in terms of a few parameters.

II. EXPERIMENTAL

$CuBr_2$, $CuCl_2$, and CuF_2 were obtained commercially, CuF_2 was packed in a sealed bottle in a nitrogen atmosphere. Only for $CuCl_2$ was it necessary to dehydrate, and this was done by heating the sample three days at 200 °C *in vacuo*. All materials were then subjected to the same procedure. They were inserted in the nitrogen-filled glovebox attached to the spectrometer, especially dried using a nitrogen-cooled copper coil. The crystals were powdered in order to expose new surfaces, free of oxygen and water. Immediately thereafter the powder was pressed onto adhesive tape and inserted into the spectrometer. The spectra were collected with an AEI ES 200 spectrometer at a pressure of 10^{-10} torr obtained with turbomolecular and Ti sublimation pumps. As a source Al or Mg $K\alpha$ radiation was used. The temperature of the sample was kept at 200 K to avoid dissociation and to prevent gassing of the adhesive tape.

Carbon and oxygen lines and also the monovalent part of the copper core lines, which are shifted from the main lines by several eV toward lower-binding energy, were simultaneously monitored. At the moment hindering amounts of monovalent copper halide were observed the measurements were stopped and repeated again with fresh material. In the case of CuF_2 it was not possible to keep a clean divalent compound for a long time which resulted in poor statistics for the clean divalent sample. Spectra were recorded of the lines given in Tables I and II. All spectra were corrected for analyzer transmission, röntgen satellites, and background by computation methods described earlier.[11] Because these materials are insulators, there will be charging of the sample. We have choosen the C 1*s* line, set at 284.6 eV, as a reference for all compounds.

TABLE II. Kinetic energies in eV of the $L_3M_{23}M_{45}$ and $L_3M_{45}M_{45}$ Augers in copper dihalides.

	CuF_2	$ClCl_2$	$CuBr_2$
$L_3M_{23}M_{45}$, ${}^3D+{}^3P$	843.0	843.1	845.1
$L_3M_{23}M_{45}$, ${}^1F+{}^1P$	834.4	835.1	836.7
$L_3M_{45}M_{45}$, ${}^1G$	914.6	915.5	917.1
$L_3M_{45}M_{45}$, satellite	909.2	910.1	911.9

III. RESULT AND DISCUSSION: PHOTOELECTRON SPECTRA

In Fig. 1 the Cu $2p$ region of the photoelectron spectra of CuF_2, $CuCl_2$, and $CuBr_2$ are shown. These closely resemble spectra of the same compounds reported in the literature.[1] The assignments of the peaks are also given according to Larsson.[7] The main peak corresponds to a final state $2p^5 3d^{10}$ and the satellites to a $2p^5 3d^9$ final state. These are nominal electron configurations which more exactly would include the hybridization with the ligand valence electrons. We will come back to this below. Because the satellite involves a ligand hole we also make this explicit in our notation and refer to the states as $\underline{2p}3d^{10}\underline{L}$ and $\underline{2p}3d^9$, where $\underline{2p}$ and $\underline{L}$ indicate that there is one electron missing in the Cu $2p$ and the ligand valence state, respectively.

We see that in $CuCl_2$ and $CuBr_2$ the satellite of the $2p_{3/2}$ line shows some structure whereas in CuF_2 both the main and satellite lines are broad. This structure is a result of multiplet splitting in the $\underline{2p}3d^9$ final state. Neglecting the crystal field in the final state we expect to see eight final states for $\underline{2p_{3/2}}\,3d^9$ and four for $\underline{2p_{1/2}}\,3d^9$ corresponding to total angular momentum $J=4, 3, 2, 1, 0$ in J-J coupling. The relative energies of these states have been calculated by Van Piggelen[12] using a relativistic numerical Fock-Dirac *ab initio* calculation. A calculation including a crystal field of D_{4h} symmetry was also done which resulted in states at almost the same energies as those neglecting the crystal field. The intensities of the lines corresponding to the various final states were calculated using fractional parentage. The result of this calculation is shown as solid bars in Fig. 2 together with the $CuCl_2$ spectrum. This splitting in the satellite is not seen in CuF_2. The $2p_{3/2}$ lines however are very broad which is not a result of different charging because the F $1s$ line is quite narrow [FWHM (full width at half maximum) is 2 eV]. That both the main and satellite lines are broad could be a result of mixing the states $\underline{2p}\,3d^9$ and $\underline{2p}\,3d^{10}\underline{L}$ which is, as we will see below, the strongest for CuF_2.

In Fig. 3 the Cu $3p$ and Cu $3s$ regions are shown, the assignment is given in the lower part of Fig. 4. It should be noticed that according to the above assignment the shoulder on the high binding-energy side of the $3s$ line is not solely due to exchange splitting[13] but rather that the width of this shoulder is due to two lines corresponding to the $\underline{3s}\,3d^9$ (^3D) and $\underline{3s}$ $3d^9(^1D)$ configurations. The exchange splitting calculated from atomic Slater integrals[14] is then expected to be 4.7 eV. For $CuBr_2$ the observed value is approximately 3.2 eV. This reduction is most probably due to $3s$-$3d$ correlation effects. It would be interesting to compare the experimental splitting with a spin-unrestricted Hartree-Fock calculation for the $\underline{3s}\,3d^9(^3D)$ and (^1D) states.

The broad satellite in the region between the Cu $3s$ and $3p$ line (marked *i* in Fig. 4) which is seen in CuF_2 and $CuCl_2$ (Fig. 3) is ascribed to an energy-loss peak since it is observed in all core as well as Auger spectra at the same energy separation of about 24 eV from the main peak. This is also the reason for the somewhat strange shape of the $CuBr_2$ spectrum (Fig. 3). Here the energy-loss peak originating from the

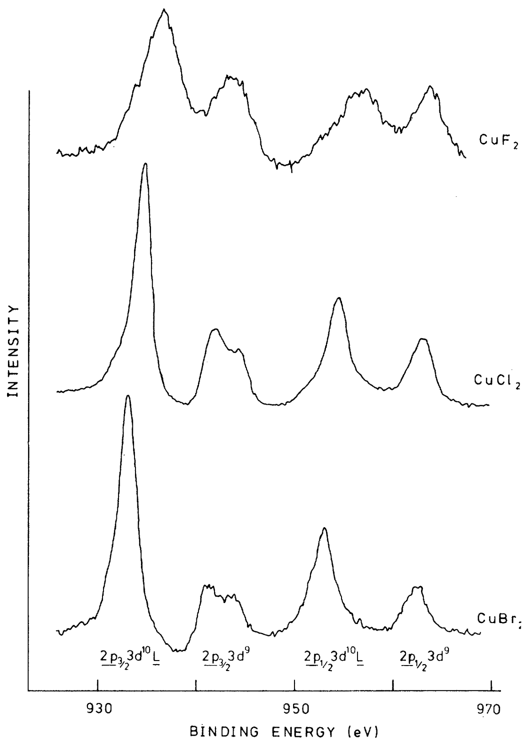

FIG. 1. Cu $2p$ photoelectron spectra of Cu dihalides. The lines leading to a final state with a ligand hole (L) show a chemical shift.

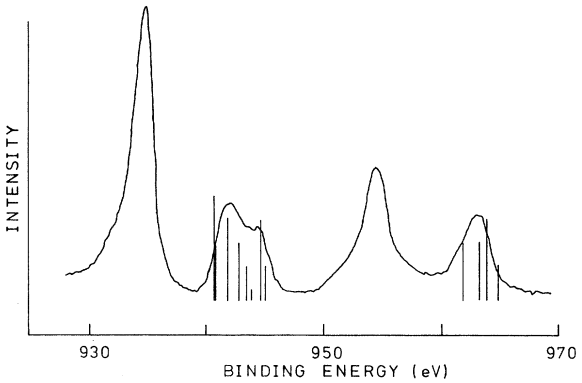

FIG. 2. The Cu $2p$ spectrum of $CuCl_2$ together with the expected multiplet splittings, represented by bars, for the $\underline{2p}3d^9$ level as calculated and discussed in the text.

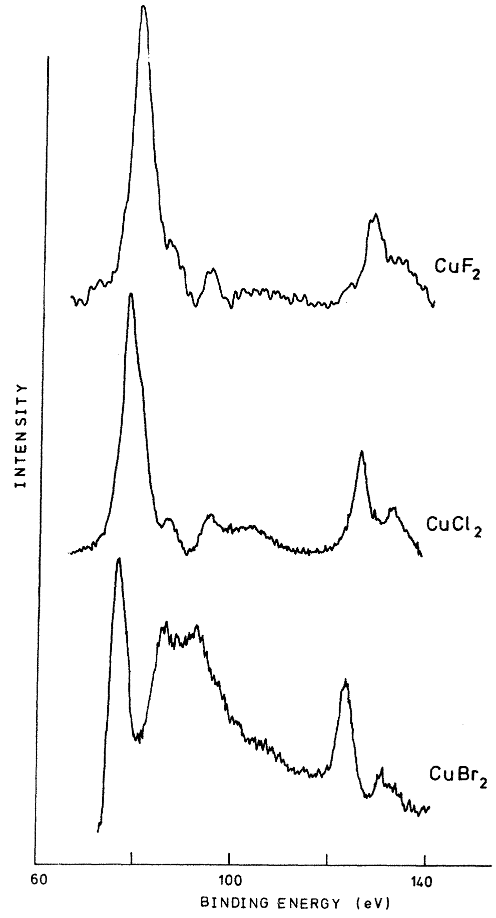

FIG. 3. The Cu $3p$ and Cu $3s$ regions of Cu dihalides. The assignment of these regions is given in the lower part of Fig. 4.

Br $3d$ photoelectron peak (binding energy $=68.7$ eV) coincides with the satellite structure on the Cu $3p$ lines.

We see that the Cu $3p$ line consists of a high-intensity line with at the high binding-energy side some small peaks. Again the main peak is assigned to $\underline{3p}3d^{10}\underline{L}$ and the satellites to $\underline{3p}3d^9$.

The valence-band region is shown in Fig. 5. Here we find the spectra of ligand outer s orbitals as indicated and the valence region which consists of ligand p orbitals and Cu $3d$ orbitals. In the monovalent compounds the ligand valence p band and the Cu $3d$ band are well separated.[15] This is not the case for these divalent compounds. The identification of the various peaks in the figure between the valence band and the ligand outer s peak will be discussed below. For a correct interpretation of the observed photoelectron energy levels it is instructive to consider also the Auger spectra.

In Table I and II all energies are listed taking as a reference a C $1s$ binding energy of 284.6 eV. We see in Table I and Figs. 1 and 2 an interesting trend. The satellite peak positions are nearly independent of the ligand whereas the main line shifts on going from CuF_2 to $CuCl_2$ to $CuBr_2$. This is especially clear from the $2p_{1/2}$ region where the spectra are not complicated by multiplet structure. In order to understand this we consider the energies involved. According to the assignment given above the main line is a result of a final state $\underline{c}d^{10}\underline{L}$, where $\underline{c}$ denotes a core hole and $\underline{L}$ a ligand hole. The energy of this final state will be given by

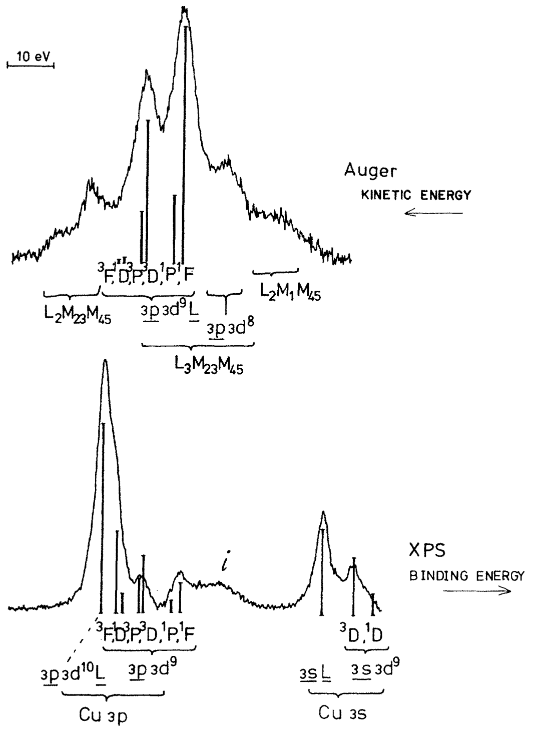

FIG. 4. Assignment of the Cu $L_{23}M_{23}M_{45}$ Auger spectra (upper part) and the Cu $3p$ and $3s$ region (lower part) of $CuCl_2$. The intensities and positions of the various terms are given by the height and separation of the bars, respectively. Here it is seen that the XPS $\underline{3p}\,3d^9$ configuration has the same term splitting as the Auger $\underline{3p}\,3d^9\underline{L}$ final state (see text). The satellite marked i is an energy-loss peak.

$$E_{\text{main}}=E(\underline{c}d^{10}\underline{L})\simeq E(\underline{c}d^{10})+E(\underline{L}) \ ,$$

where we have neglected the interaction between the ligand hole and the electrons or holes on the copper ion. The energy of the satellite line is given by

$$E_{\text{sat}}=E(\underline{c}d^9) \ .$$

From this we see that if the same reference level is used for all materials the satellite peak position will in first approximation be independent of the ligand. The small changes in energy (see Table I) are due to differences in extra-atomic relaxation as a result of

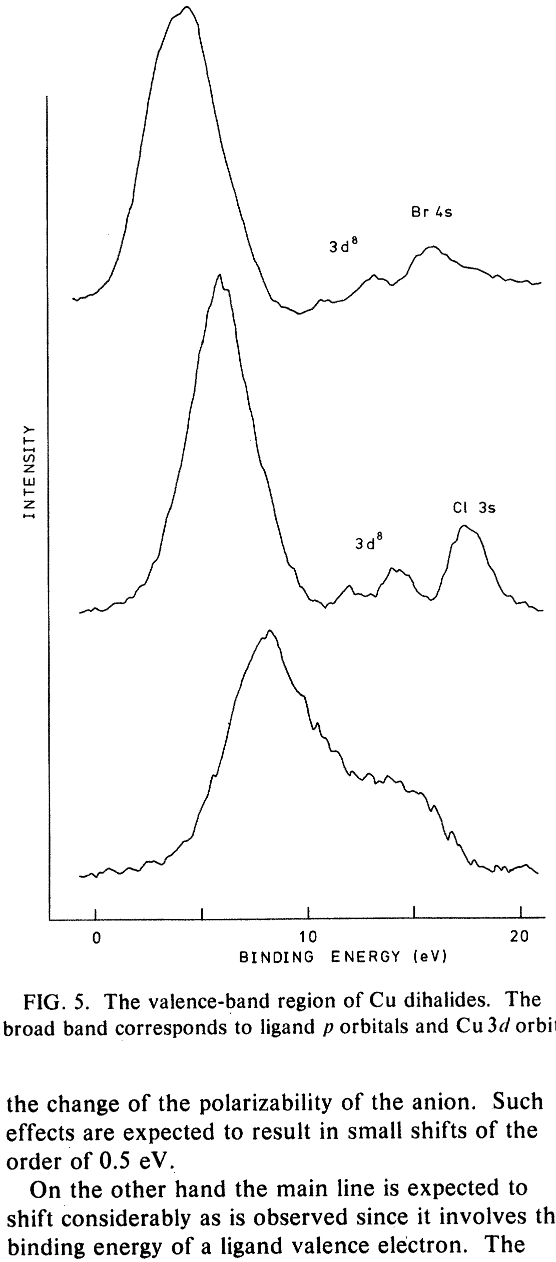

FIG. 5. The valence-band region of Cu dihalides. The broad band corresponds to ligand p orbitals and Cu $3d$ orbitals.

the change of the polarizability of the anion. Such effects are expected to result in small shifts of the order of 0.5 eV.

On the other hand the main line is expected to shift considerably as is observed since it involves the binding energy of a ligand valence electron. The ligand binding energy is expected to decrease in going from the fluoride to the bromide by about 3 eV as can be deduced from zinc dihalide results listed in Table III. We see that the Cu $2p$ main line binding energy in the Cu dihalides closely follows the valence ligand binding energy in the Zn dihalides.

In the above we have implicitly assumed that there is no hybridization or mixing of the states $\underline{c}3d^{10}\underline{L}$ and $\underline{c}3d^9$. These states can mix but because of the large Coulomb interaction between the core hole and the $3d$ hole, these states are well separated in energy and the mixing can in first approximation be neglected. This approximation cannot be made when considering intensities, as will be seen below.

A. $L_3M_{23}M_{45}$ Auger spectra

We will now try to show that the peak assignments at least for the core lines are indeed correct. We consider the Cu $L_{23}M_{23}M_{45}$ Auger transition. If the assignment of the main Cu $2p_{3/2}$ line is correct the main

TABLE III. Experimental binding energies in eV of zinc dihalides valence band with C $1s$ at 284.6 eV.

	Zn $3d$	Ligand valence p
ZnF_2	11.6	7.5 *a* 8.0
$ZnCl_2$	12.0	5.7
$ZnBr_2$	12.0	4.9

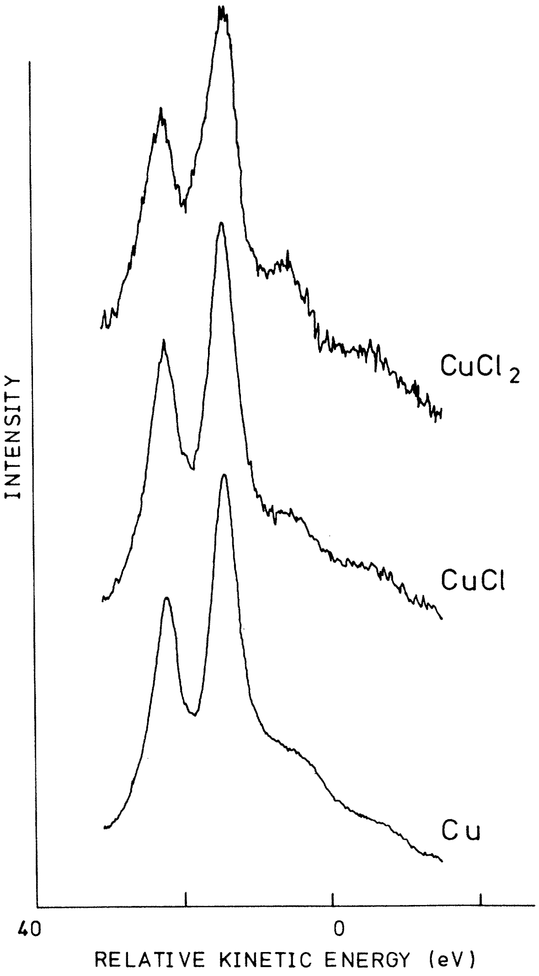

FIG. 6. The Cu $L_3M_{23}M_{45}$ Auger spectra of $CuCl_2$, CuCl, and Cu metal. The assignment of the spectra is given in the upper part of Fig. 4.

part of the Auger transition will originate from a $2\underline{p}3d^{10}\underline{L}$ with one hole in the ligand orbitals. The main Auger spectrum should then look much like that of Cu metal. In Fig. 6 the Auger spectrum of $CuCl_2$ is shown together with that of CuCl and Cu metal. We see indeed that these Auger transitions are very similar showing approximately the same multiplet structure. The linewidths are different and the satellite (shown at a relative kinetic energy of about 8 eV in Fig. 6) is much stronger in $CuCl_2$ than in CuCl or Cu metal. For Cu metal this satellite is attributed to a Coster-Kronig-preceded Auger transition[15,16] resulting in a final state $3\underline{p}3d^8$. That this satellite is enhanced in $CuCl_2$ is because in addition to the Coster-Kronig transition we can also obtain a $3\underline{p}3d^8$ final state starting with a $2\underline{p}3d^9$ initial state. This initial state corresponds to the satellite observed in the Cu $2p$ spectrum of $CuCl_2$ (Fig. 1). The same kind of effect is seen in the $L_{23}M_{45}M_{45}$ regions of the Auger spectra shown in Fig. 7.

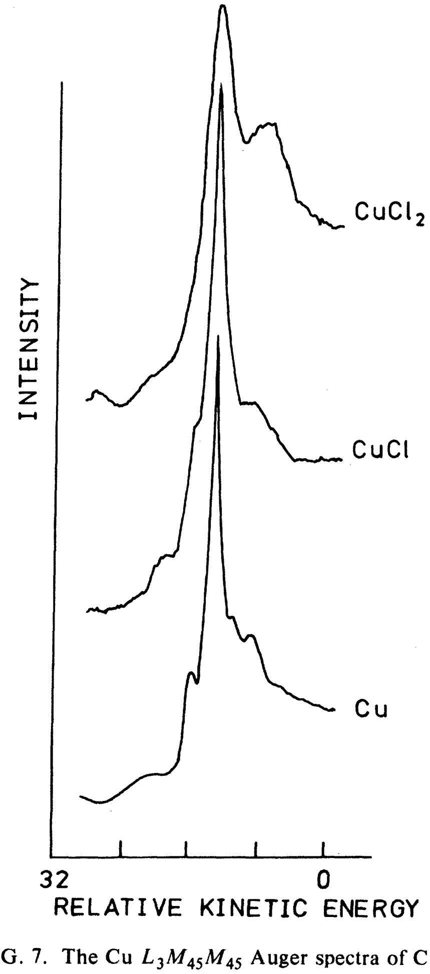

FIG. 7. The Cu $L_3M_{45}M_{45}$ Auger spectra of $CuCl_2$, CuCl, and Cu metal. The assignment of the spectra is the same as in Fig. 11.

The validity of the assignment for the $3p$ lines as shown in Fig. 4 can be proved more rigorously. The main line corresponds to the final state $3\underline{p}d^{10}\underline{L}$ and the satellite to $3\underline{p}d^9$. The latter is at least locally the same state reached by the $L_{23}M_{23}M_{45}$ Auger process. The main Auger line originates from $2\underline{p}d^{10}\underline{L}$ decaying to the final state $3\underline{p}d^9\underline{L}$. The only difference between this final state and the $3p$ satellite is the presence of an extra ligand hole. The energy of the Auger final state is given by

$$E(3\underline{p}d^9\underline{L}) \simeq E(3\underline{p}d^9) + E(\underline{L}) \ , \qquad (1)$$

again neglecting the interaction between the ligand hole and the Cu holes. The Auger kinetic energy is then given by

$$\begin{aligned} E_K(L_3M_{23}M_{45}) &= E(2\underline{p}_{3/2}d^{10}\underline{L}) - E(3\underline{p}d^9\underline{L}) \\ &= E(2\underline{p}_{3/2}d^{10}\underline{L}) - E(3\underline{p}d^9) - E(\underline{L}) \end{aligned} \qquad (2)$$

from which we obtain

$$E(3\underline{p}3d^9) = E(2\underline{p}_{3/2}3d^{10}\underline{L}) - E(\underline{L}) - E_K(L_3M_{23}M_{45}) \ .$$

The quantities $E(2\underline{p}_{3/2}3d^{10}\underline{L})$ and E_K $(L_3M_{23}M_{45})$ are both measured quantities, the former corresponding to the binding energy of the main $2p_{3/2}$ line. The binding energy $E(\underline{L})$ is more difficult to obtain as will be discussed below. The main point is that the final state obtained in Auger and in the Cu $3p$ satellite spectrum should have the same multiplet splitting and should be shifted by $E(\underline{L})$ with respect to each other. The possible final states for a configuration $3\underline{p}3d^9$ are ^1F, ^1P, ^3D, ^3P, ^1D, and ^3F. The energies expressed in eV are given in terms of the Slater integrals by

$$\begin{aligned}
{}^1F &= E^0 + F^0 + \tfrac{2}{35}F^2 + \tfrac{6}{15}G^1 + \tfrac{3}{245}G^3 = E^0 + F^0 + 7.39 \ , \\
{}^1P &= E^0 + F^0 + \tfrac{7}{35}F^2 + \tfrac{1}{15}G^1 + \tfrac{63}{245}G^3 = E^0 + F^0 + 5.36 \ , \\
{}^3D &= E^0 + F^0 - \tfrac{7}{35}F^2 + \tfrac{3}{15}G^1 - \tfrac{21}{245}G^3 = E^0 + F^0 - 0.22 \ , \\
{}^3P &= E^0 + F^0 + \tfrac{7}{35}F^2 - \tfrac{1}{15}G^1 - \tfrac{63}{245}G^3 = E^0 + F^0 - 1.02 \ , \\
{}^1D &= E^0 + F^0 - \tfrac{7}{35}F^2 - \tfrac{3}{15}G^1 + \tfrac{21}{245}G^3 = E^0 + F^0 - 5.11 \ , \\
{}^3F &= E^0 + F^0 + \tfrac{2}{35}F^2 - \tfrac{6}{15}G^1 - \tfrac{3}{245}G^3 = E^0 + F^0 - 6.24 \ .
\end{aligned}$$

In these expressions E^0 is the energy of the state $3\underline{p}3d^9$ in the absence of Coulomb interactions. Taking atomic Slater integrals for $3p$-$3d$ from Mann[14] $F^2 = 13.34$, $G^1 = 16.53$, and $G^3 = 9.94$ eV, we obtain the values given on the right-hand side. The calculated positions and intensities of the final-state terms are given as vertical lines in Fig. 4. The Auger intensities are calculated using McGuire's radial integrals.[17,18]

The comparison between the $L_{23}M_{23}M_{45}$ Auger spectra and the $3p$ satellite spectra is shown in Fig. 4. From Eq. (2) the additional shifts due to $E(\underline{L})$ are determined, and values of 8.2, 5.3, and 3.5 eV of $E(\underline{L})$ are calculated for the fluoride, chloride, and bromide, respectively. (See Fig. 8.) This shows the expected trend in the ligand valence-orbital binding energies. The differences here are slightly larger than those obtained above from the Cu $2p$ main-line binding energies which reflects the Coulomb interaction between the ligand orbital and the two-hole $\underline{3p}3d^9$ configuration as well as small shifts due to hybridization. Since however the term splittings are close to the free atom values the hybridization cannot be very strong.

We notice from Fig. 4 that the final states ^3F and ^1D which have a low intensity in the Auger spectrum are expected to coincide nearly in energy with the $3p$ main line in the $3p$ XPS spectrum. The relative intensities of the various final-state terms in the $3p$ photoelectron spectrum are determined by the overlap integral

$$I(\chi)=\sum|\langle 3p,d_{x^2-y^2}|\chi\rangle|^2 ,$$

where the sum is over all frozen states $3p,d_{x^2-y^2}$ and over the degenerate states in the final-state term χ. $d_{x^2-y^2}$ is the B_{1g} orbital of the initial state. Since the term splitting in the final state is much larger than the crystal-field splitting we can neglect the latter. For this case the intensities are simply proportional to the multiplicity of the final-state terms. We therefore expect the satellite intensities to be in the ratio of 7:3:15:9:5:21 for the ^1F, ^1P, ^3D, ^3P, ^1D, ^3F, respectively, with the terms ^1D and ^3F coinciding nearly in energy with the main peak. These are the intensity ratios expected for equal mixing of the various final-state terms with states with a ligand hole. We will come back to the problem of mixing below.

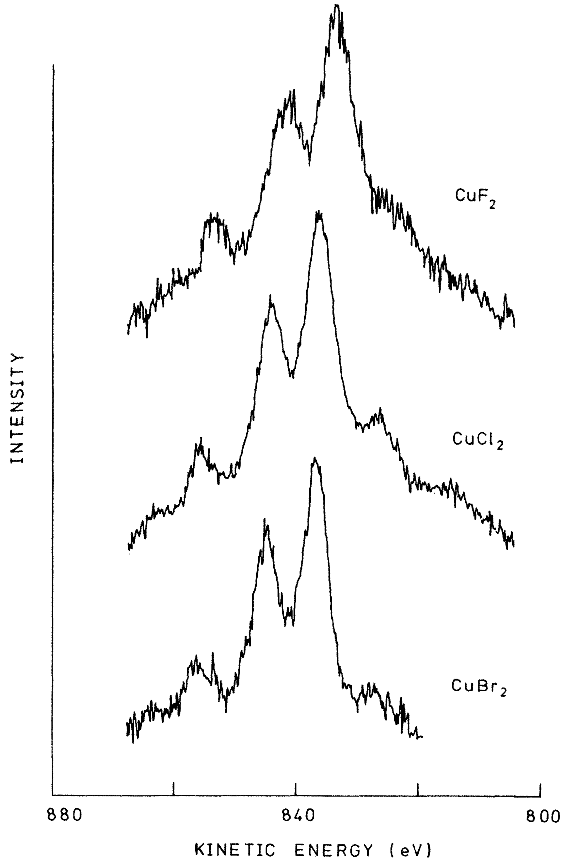

FIG. 8. The Cu $L_3M_{23}M_{45}$ Auger spectra of CuF$_2$, CuCl$_2$, and CuBr$_2$. The assignment of the spectra is given in the upper part of Fig. 4.

B. Valence band and $L_3M_{45}M_{45}$ Auger spectra

Making use of the identification of the satellites of the core lines, and the determination of the valence ligand binding energies an interpretation of the valence bands shown in Fig. 5 becomes possible.

Since hybridization of the $\underline{3p}3d^9$ state with the $\underline{3p}3d^{10}\underline{L}$ state is small at least for the well-split-off ^1P and ^1F terms, the ligand binding energies determined above are those corresponding to zero hybridization. (See Fig. 9.) This is not the case for the states involved in the valence-band region because here hybridization will be important. After removal of a valence electron a Cu L_6 cluster will have two holes. We should therefore consider all possible final states with two holes in the valence shell in a calculation of the energies and intensities. These are three distinctly different two-hole states corresponding to d^8, $d^9\underline{L}$, $d^{10}\underline{L}^2$ (Fig. 10). The energy of the d^8 state can be obtained from the $L_{23}M_{45}M_{45}$ Auger spectrum shown in Fig. 11 and the kinetic energies given in Table II.

The $L_{23}M_{45}M_{45}$ Auger spectra of the Cu dihalides are similar to those of Cu metal and Cu monohalide except that they are broadened probably mainly due to crystal-field splitting (which results in a splitting of the ^1G, ^3P, ^1D, and ^3F final-state terms) (see Fig. 7). The peaks marked A in the $L_3M_{45}M_{45}$ Auger spectra are most likely due to final states $3d^9\underline{L}^2$ which can be reached because of covalent mixing with the states $3d^8\underline{L}$. This is similar to the peak seen in the monochloride (Fig. 7) discussed recently.[15] The observed decrease in intensity of the peaks on going from the difluoride to the dibromide is consistent with the expected decrease in the mixing because of the increase in splitting of the $d^9\underline{L}^2$ and $d^8\underline{L}$ peaks. This increase in splitting is caused by the decrease in the ligand hole energies as discussed above.

We remark that one expects two separate peaks $3d^9\underline{L}^2$ corresponding to states with the two ligand holes at the same or at different ligand atoms, with for zero hybridization a probability ratio $1/(N-1)$, where N is the number of ligand neighbors of the Cu atom.[19]

The satellite at the low kinetic energy side in these

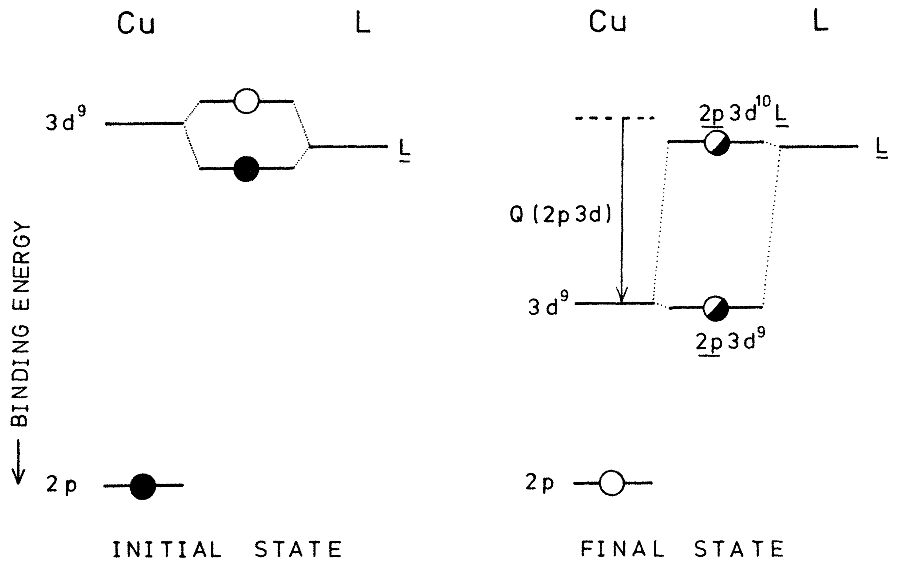

FIG. 9. Schematic picture of the initial state and the final state for the Cu $2p$ photoelectron spectrum. In the final state the Cu $3d^9$ energy level is lowered due to the Coulomb interaction Q $(2p3d)$ with the $2p$ core hole (●: electron, ○: hole, ◐: partly filled).

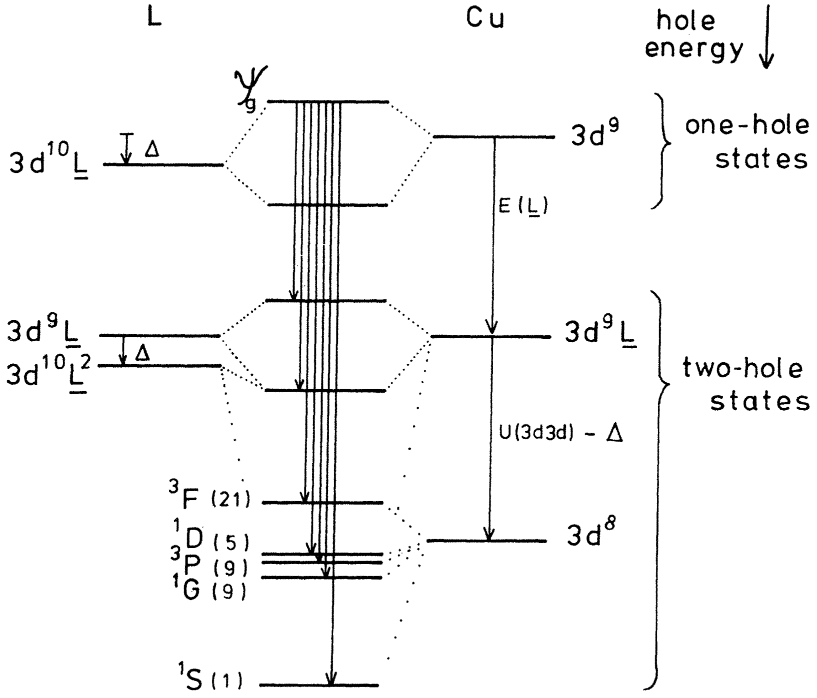

FIG. 10. Diagram with the transitions that occur in the valence band of Cu dihalides, going from the one-hole initial state to the two-hole final states. The various possible $\underline{L}^2$ states have been represented by one line.

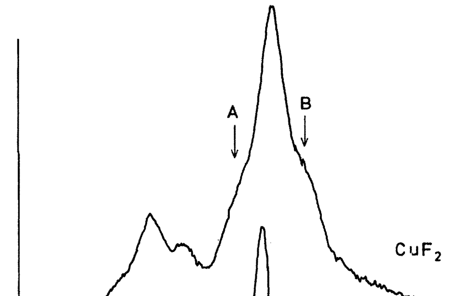

FIG. 11. Cu $L_{23}M_{45}M_{45}$ Auger spectra of Cu dihalides. A is a $3d^2\underline{L}^9$ final state and B is a $3d^7$ final state as discussed in the text. i is an energy-loss peak.

spectra, marked as B, comes at about the same position as the Koster-Kronig-preceded Auger transition in Cu (Refs. 15 and 16) but is much more intense. This is due to an Auger transition originating from the $2p$ final state. The main line originates from a $\underline{2p}3d^{10}\underline{L}$ state and ends in a $3d^8\underline{L}$ state (neglecting interatomic Auger processes which are very weak). The kinetic energy of main line and this satellite in the Auger spectrum are given by

$$E_K(M)=E(\underline{2p}3d^{10}\underline{L})-E(3d^8\underline{L}) \ ,$$

$$E_K(S)=E(\underline{2p}3d^9)-E(3d^7) \ .$$

The energy splitting between main and satellite line is given by

$$E_K(M)-E_K(S)=E(\underline{2p}3d^{10}\underline{L})-E(\underline{2p}3d^9)+E(3d^7)-E(3d^8\underline{L}) \ .$$

As discussed in the interpretation of the core levels the satellite-main peak splitting of the $2p$ spectrum varies approximately as the ligand valence binding energy. This is also expected to be the case for $E(3d^7)-E(3d^8\underline{L})$ thereby canceling the ligand valence-electron contribution arising from the first two terms. The Auger satellite main-peak splitting is then given approximately by

$$E_K(M)-E_K(S)\simeq 2U(3d,3d)-Q(2p,3d) \ , \quad (3)$$

where $U(3d,3d)$ is the Coulomb interaction between two $3d$ holes and $Q(2p,3d)$ the Coulomb interaction between the $2p$ hole and a $3d$ hole on the same Cu atom. One would also expect on the right-hand side of the equation, quantities like $Q(L,2p)$ and $Q(L,3d)$, representing the Coulomb interaction between a hole on the ligand atom and a $2p$ hole or a $3d$ hole, respectively. However, these interatomic Coulomb interactions are much more effectively shielded than the intra-atomic Coulomb interactions.[20]

From the main Auger line we can directly determine the energy of the $3d^8\underline{L}$ state

$$E(3d^8\underline{L})=E(\underline{2p}_{3/2}3d^{10}\underline{L})-E_K(L_3M_{45}M_{45}) \ .$$

Because of the large $3d$-$3d$ Coulomb interaction (≈ 8 eV) the $3d^8\underline{L}$ state will hardly hybridize with d^7 or $d^9\underline{L}^2$ (except for CuF$_2$). Therefore the energy of the d^8 state can be determined by subtracting the ligand binding energy

$$E(3d^8\underline{L})\approx E(3d^8)+E(\underline{L}) \ . \quad (4)$$

As was calculated from the energy positions of the inner electrons and as is seen in Fig. 5, the energy of the $3d^8$ structure is approximately the same in all three Cu dihalides, due to the fact that in this state the ligand valence orbitals are all completely filled. However the $3d^9\underline{L}$ state will shift from one ligand to another in the same manner as the core $\underline{c}3d^{10}\underline{L}$ and the $3d^{10}\underline{L}^2$ will shift twice as much.

As is drawn in Fig. 10, if we neglect hybridization, the $3d^9\underline{L}$ is a distance $U(3d3d)-\Delta$ and the $3d^{10}\underline{L}^2$ a distance $U(3d3d)-2\Delta-U(LL)$ separated from the $3d^8$ level, where the U's are Coulomb integrals and Δ is the energy distance between the unhybridized $3d^9$ and $3d^{10}\underline{L}$ one-hole states. From atomic-cross-section calculations[21] we find, for the fluoride, chloride, and bromide that 14%, 32%, and 53%, respectively, of the intensity in the valence band is due to emission from a ligand p orbital. Although binding effects have an important influence on these numbers, it is clear that both $3d^9\underline{L}$ and $3d^{10}\underline{L}^2$ will contribute to the spectrum, so these lines nearly coincide.

From Table I is seen that the distance $3d^9\underline{L}-3d^8$ (average) is about 1 eV smaller than the $2p_{1/2}$ main satellite splitting. This gives an indication for

$U(3d3d)$ and $Q(2p,3d)$. A detailed calculation for these Coulomb integrals can be done with Eq. (3) together with the differences in the Auger kinetic energy of the three-hole final states and the energies of the two-hole final states obtained from XPS. This gives a value for $Q(2p3d)$ of about 5 to 8 eV and for $U(3d3d)$ of about 5 to 7 eV. This agrees well with the observed splitting between valence band and main $3d^8$ satellite.

C. Satellite intensities

We now turn to the problem of satellite intensities. The eigenstates in the initial state are linear combinations of $\psi(3d^9)$ and $\psi(3d^{10}\underline{L})$ with the hole in a B_{1g} orbital of the D_{4h} point group. By taking

$$\Delta = E(3d^{10}\underline{L}) - E(3d^9)$$

and a mixing matrix element of the Hamiltonian H given by

$$T = \langle \psi(3d^9) | H | \psi(3d^{10}\underline{L}) \rangle \tag{5}$$

and neglecting overlap, the eigenvalues are

$$E_{1,2} = E_0 + \tfrac{1}{2}\Delta \pm \tfrac{1}{2}(\Delta^2 + 4T^2)^{1/2} \ . \tag{6}$$

For a positive value of T the corresponding eigenfunctions can be written as

$$\psi_1 = \sin\theta\psi(3d^9) + \cos\theta\psi(4d^{10}\underline{L}) \ ,$$

$$\psi_2 = \cos\theta\psi(3d^9) - \sin\theta\psi(3d^{10}\underline{L}) \ ,$$

with

$$\tan 2\theta = 2T/\Delta \tag{7}$$

and the value of θ restricted to $0 < \theta < 90°$.

For the final state with a core hole on the copper we have to take into account the interaction Q of the core hole with the $3d^9$ state. The eigenvalues are

$$E_{s,m} = E_0' + \tfrac{1}{2}\Delta \pm \tfrac{1}{2}[(\Delta - Q)^2 + 4T^2]^{1/2} \tag{8}$$

with the corresponding eigenfunctions

$$\psi_1 = \sin\theta'\psi(\underline{c}3d^9) + \cos\theta'\psi(\underline{c}3d^{10}\underline{L}) \ ,$$

$$\psi_m = \cos\theta'\psi(\underline{c}3d^9) - \sin\theta'\psi(\underline{c}3d^{10}\underline{L}) \ ,$$

with

$$\tan 2\theta' = 2T/(\Delta - Q) \tag{9}$$

and the value of θ' restricted to $0 \leqslant \theta' \leqslant 90°$. The photoelectron spectrum will consist of a main peak with intensity I_m corresponding to the final state of lowest energy E_m and a satellite corresponding to the final-state energy E_s. The energy separation between the main and satellite peaks is

$$W = E_s - E_m = [(\Delta - Q)^2 + 4T^2]^{1/2} \ . \tag{10}$$

In the sudden approximation the intensity ratio of the satellite and main peaks is given by

$$\frac{I_s}{I_m} = \left[\frac{\sin\theta'\cos\theta - \cos\theta'\sin\theta}{\cos\theta'\cos\theta + \sin\theta'\sin\theta} \right]^2 = \tan^2(\theta' - \theta) \ . \tag{11}$$

From the choice of the wave functions above, it follows that $0 < \theta < 45$ for $\Delta > 0$ and $45 < \theta < 90$ for $\Delta < 0$ and $0 < \theta' < 45$ for $\Delta - Q > 0$ and $45 < \theta' < 90$ for $\Delta - Q < 0$.

The satellite intensity therefore depends only on the difference in hybridization between the initial and final state. From Table IV and Fig. 1 we see that the satellite intensity is high showing that there must be an appreciable change in hybridization. Using Eq. (11) we find that $|\theta' - \theta|$ is 41.8°, 37.8°, and 33.9° for the fluoride, chloride, and bromide, respectively.

From Eqs. (7), (9), (10), and (11) we obtain

$$\pm 2\arctan(I_s/I_m)^{1/2} = \arcsin(2T/W) - \arctan(2T/\Delta) \tag{12}$$

$$\pm \text{ for } \theta' - \theta \lessgtr 0 \ .$$

There are three unknown quantities T, Δ, and Q in this equation and only two experimentally determined quantities I_s/I_m and W. In Fig. 12 we have plotted the values of Δ and Q as a function of T using experimental values for I_s/I_0 and W. It is difficult to estimate the actual values of T although $(\Delta^2 + 4T^2)^{1/2}$ must be smaller than the experimental width of the valence band. If we assume that the $2p$-$3d$ Coulomb interaction does not vary much for the different dihalides we find from Fig. 12 that T lies between 2 and 2.5 eV. For $CuBr_2$ we see that Δ is little different from zero suggesting strong hybridization.

To get an indication of the amount of hybridization in the initial and final state we have plotted in Fig. 13, $\cos^2\theta$ and $\cos^2\theta'$ as a function of T again using the experimental values for I_s/I_m and W. This is the amount of $3d^9$ character in the initial ground state and the lowest-lying final state, respectively. We see that the lowest-lying final state is indeed mainly $3d^{10}\underline{L}$ ($\cos^2\theta' < 0.5$) and the initial ground state is

TABLE IV. Satellite main peak separation W in eV and satellite main peak intensity ratio I_s/I_m in the copper dihalides, measured on the Cu $2P_{1/2}$ structure.

	W	I_s/I_m
CuF_2	7.0	0.8
$CuCl_2$	8.8	0.6
$CuBr_2$	10.0	0.45

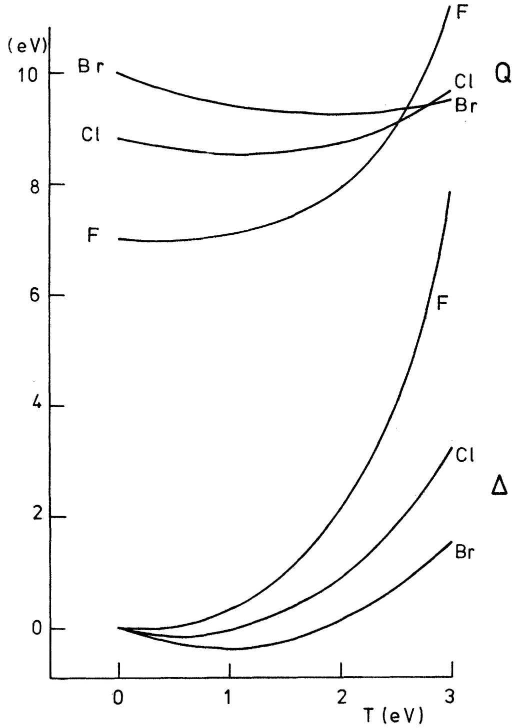

FIG. 12. Possible solutions of Eq. (12) for Δ and $Q(2p3d)$ for the observed values of I_s/I_m and W, when T is continuously varied between 0 and 3 eV.

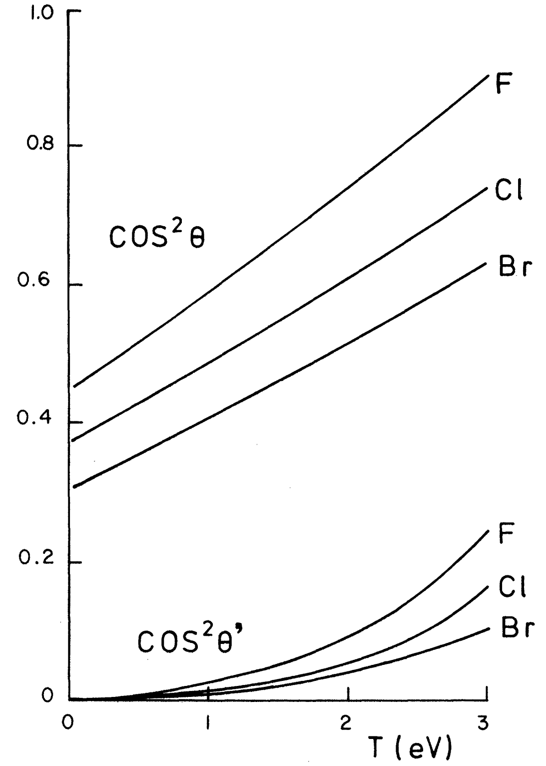

FIG. 13. The amount of $3d^9$ character in the ground state $\cos^2\theta$ and the amount of $\underline{2p}3d^9$ character in the lowest final state $\cos^2\theta'$, calculated with Eq. (12) from the observed values of I_s/I_m and W, when T is continuously varied between 0 and 3 eV.

quite strongly hybridized. Also the hybridization of the ground state increases on going from the fluoride to the bromide which is consistent with a decrease in electronegativity. The reason that $\cos\theta$ does not go to zero as $T \rightarrow 0$ is that Δ and Q then vary in such a way that I_s/I_m and W remain equal to the experimental values.

It is possible in principle to extract the same information from the satellite intensities of the other core lines of Cu, but the $2p_{1/2}$ line is the most suitable one, because the term splitting in the satellite is small and the two final states are well separated because the Coulomb integral is large.

For the satellite intensities in the valence band the situation is quite different. Figure 5 shows that the intensity of the $3d^8$ satellite in $CuCl_2$ and $CuBr_2$ is strongly reduced. The difference in intensity could be due to the fact that in the core satellite the same one-electron transfer integral can be taken for the initial state as well as for the final state when the core hole is localized:

$$T = \langle \underline{c}3d^9 | H | \underline{c}3d^{10}\underline{L} \rangle \approx \langle 3d^9 | H | 3d^{10}\underline{L} \rangle \ .$$

But this is not so for the transfer integral in the valence-band satellites. For the valence-band satellites we must consider the covalent mixing of a state $3d^8$ with strong term splittings with a state $3d^9\underline{L}$ with small term splittings. The matrix element connecting these states is expected to be considerably smaller than T. Also we notice from Fig. 5 that for $CuCl_2$ and $CuBr_2$ the $3d^8$ state is not far removed from the ligand s "core state." There may therefore be quite strong hybridization with the $3d^9\underline{Ls}$ state. With these complications it is difficult to estimate the intensity expected.

IV. CONCLUSIONS

Using a combination of XPS and Auger spectroscopy we have made a clear assignment of the XPS main and satellite peaks of CuF_2, $CuCl_2$, and $CuBr_2$. A simple model calculation is used to relate the satellite intensities and peak positions to the initial- and final-state hybridization. It is shown that $CuCl_2$ and especially $CuBr_2$ are strongly covalent. Extrapolation to CuI_2 leads to the conclusion that here the I $5p$ hole state would be lower in energy than the Cu $3d$ hole state, suggesting that CuI_2 would be unstable, according to the reaction $Cu^{++} + 2I^- \rightarrow Cu^+I^- + I$. Using the core line and Auger results the valence-band spectra can be clearly interpreted. These spectra cannot be understood in terms of a one-particle picture because of the strong $3d$-$3d$ Coulomb interactions. The $3d^8$ final states are clearly observed in the valence-band region and they should show the same resonances as observed in Ni metal.[22]

ACKNOWLEDGMENTS

This work was performed as part of the research programs of the Stichting voor Scheikundig Onderzoek Nederland (SON) with financial support from the Nederlandse Organisatie voor Zuiver Wetenschappelijk Onderzoek (ZWO).

---

[1] D. C. Frost, A. Ishitani, and C. A. McDowell, Mol. Phys. 24, 861 (1972).

[2] R. Manne and T. Åberg, Chem. Phys. Lett. 7, 282, (1970).

[3] L. Yin, I. Adler, T. Tsang, L. J. Matienzo, and S. O. Grim, Chem. Phys. Lett. 24, 81 (1974).

[4] B. Wallbank, I. G. Main, and C. E. Johnson, J. Electron Spectrosc. Relat. Phenom. 5, 259 (1974).

[5] K. S. Kim, J. Electron Spectrosc. Relat. Phenom. 3, 217 (1974).

[6] Sven Larsson, Chem. Phys. Lett. 40, 362 (1976).

[7] Sven Larsson and Manuel Braga, Chem. Phys. Lett. 48, 596 (1977).

[8] A. Kotani and Y. Toyozawa, J. Phys. Soc. Jpn. 35, 1073, 1082 (1973).

[9] S. Asada and S. Sugano, J. Phys. Soc. Jpn. 41, 1291 (1976).

[10] R. P. Gupta and S. K. Sen, Phys. Rev. B 10, 71 (1974).

[11] E. Antonides, Ph.D. thesis (Laboratory of Physical Chemistry, Groningen, The Netherlands, 1977) (unpublished).

[12] H. U. Van Piggelen (private communication).

[13] C. S. Fadley and D. A. Shirley, Phys. Rev. A 2, 1109 (1970).

[14] J. B. Mann, Los Alamos Scientific Laboratory Report No. LASL-3690 (unpublished).

[15] G. van der Laan, G. A. Sawatzky, C. Haas, and H. W. Myron, Phys. Rev. B 20, 4287 (1979).

[16] H. W. Haak, G. A. Sawatzky, and T. D. Thomas, Phys. Rev. Lett. 41, 1825 (1978).

[17] V. O. Kostroun, M. H. Chen, and B. Crasemann, Phys. Rev. A 3, 533 (1971).

[18] E. J. McGuire, Sandia Laboratory Report No. SCRR-710075 (unpublished).

[19] P. H. Citrin, J. E. Rowe, and S. B. Christman, Phys. Rev. B 14, 2642 (1976).

[20] G. A. Sawatzky and D. Post, Phys. Rev. B 20, 1546 (1979).

[21] J. H. Scofield, J. Electron Spectrosc. Relat. Phenom. 8, 129 (1976).

[22] C. Guillot, Y. Ballu, J. Paigné, J. Lecante, K. P. Jain, P. Thiry, R. Pinchaux, Y. Pétroff, and L. M. Falicov, Phys. Rev. Lett. 39, 1632 (1977).